ANALYSES OF SIZE EFFECTS IN THE CHARPY V-NOTCH TEST

A.A. Benzerga[1,2], R. Batisse[1], A. Needleman[2] and V. Tvergaard[3]
[1]Gaz de France, 361 Avenue du Président Wilson, La Plaine Saint–Denis 93211, France.
[2]Brown University, Division of Engineering, Providence, RI 02912, USA.
[3]Department of Solid Mechanics, The Technical University of Denmark,
2800 Lyngby, Denmark.

ABSTRACT

This paper addresses some issues related to the size dependence of both the upper shelf energy (USE) and the ductile–brittle transition temperature (DBTT) in the Charpy V-notch test. Two classes of pipe materials are considered. Emphasis is placed on the interplay between inertial, rate hardening and thermal softening effects. In a relatively high strength pipe steel, experimental results exhibit no size dependence of the DBTT. On the other hand, a significant shift in DBTT is obtained in a low strength steel. The difference between these two classes of steels is modeled. Calculations are carried out for Charpy specimens where only the ligament size is varied, as in available experiments. The extent to which the size effect is material dependent is investigated.

KEYWORDS

Impact loading, high strain-rate, adiabatic heating, ductile-brittle transition

INTRODUCTION

The absorbed energy versus temperature or strain rate in the Charpy V-notch test is often used to characterize the ductile-brittle transition in steels. Brittle fracture is found at lower temperatures and higher strain rates while ductile fracture occurs at higher temperatures and lower strain rates. The change from the lower shelf to the upper shelf with increasing temperature is mainly a result of the variation of flow strength with temperature, while the more brittle behavior under impact loading than under slow loading results from the material strain rate sensitivity. The basic issue investigated here is the extent to which the DBTT measured in the Charpy V-notch test is a material property or a structural property that depends on specimen size and geometry.

THEORY

A convected coordinate Lagrangian formulation is used with the dynamic principle of virtual work written as

$$\int_V \tau^{ij}\delta E_{ij}\,dV = \int_S T^i \delta u_i\,dS - \int_V \rho\frac{\partial^2 u^i}{\partial t^2}\,\delta u_i\,dV \tag{1}$$

$$\text{with} \qquad T^i = (\tau^{ij} + \tau^{kj}u^i_{,k})\nu_j \tag{2}$$

$$E_{ij} = \frac{1}{2}(u_{i,j} + u_{j,i} + u^k_{,i}u_{k,j}) \tag{3}$$

where τ^{ij} are the contravariant components of Kirchhoff stress on the deformed convected coordinate net ($\tau^{ij} = J\sigma^{ij}$, with σ^{ij} being the contravariant components of the Cauchy stress and J the ratio of current to reference volume), ν_j and u_j are the covariant components of the reference surface normal and displacement

vectors, respectively, ρ is the mass density, V and S are the volume and surface of the body in the reference configuration, and $(\,)_{,i}$ denotes covariant differentiation in the reference frame.

The constitutive framework is that for a progressively cavitating porous plastic solid, with the rate of deformation tensor written as the sum of an elastic part, $\mathbf{d}^e$, a viscoplastic part, $\mathbf{d}^p$, and a part due to thermal straining, $\mathbf{d}^\Theta$, so that

$$\mathbf{d} = \mathbf{d}^e + \mathbf{d}^p + \mathbf{d}^\Theta \tag{4}$$

Small elastic strains are assumed and the elastic and thermal properties are chosen to have representative values for steel; $E = 210$ GPa, $\nu = 0.3$ and $\alpha = 1 \times 10^{-5}/^\circ$K. The viscoplastic part of the rate of deformation, $\mathbf{d}^p$, is obtained from the flow potential (Gurson [1]; Pan *et al.* [2]),

$$\Phi = \frac{\sigma_e^2}{\bar{\sigma}^2} + 2q_1 f^* \cosh\left(\frac{3q_2\sigma_h}{2\bar{\sigma}}\right) - 1 - (q_1 f^*)^2 = 0 \tag{5}$$

where $\bar{\sigma}$ is the matrix flow strength, σ_e is the Mises effective stress, σ_h is the mean normal stress and q_1, $q_2 = 1.0$ are parameters introduced in [3, 4]. The function f^*, [5], accounts for the effects of rapid void coalescence at failure

$$f^* = \begin{cases} f & f < f_c \\ f_c + (f_u^* - f_c)(f - f_c)/(f_f - f_c) & f \geq f_c \end{cases} \tag{6}$$

where f is the void volume fraction. The constant $f_u^* = 1/q_1$ is the value of f^* at zero stress. As $f \to f_f$, $f^* \to f_u^*$ and the material loses all stress carrying capacity. For a power law strain rate hardening matrix

$$\dot{\bar{\epsilon}} = \dot{\bar{\epsilon}}_0 \left(\frac{\bar{\sigma}}{g(\bar{\epsilon}, \Theta)}\right)^{1/m} \qquad g(\bar{\epsilon}, \Theta) = \sigma_0 G(\Theta) \left[1 + \frac{\bar{\epsilon}}{\epsilon_0}\right]^N \tag{7}$$

The function $g(\bar{\epsilon}, \Theta)$ represents the effective stress *versus* effective strain response in a tensile test carried out at a strain rate $\dot{\bar{\epsilon}} = \dot{\bar{\epsilon}}_0$ and m is the strain rate hardening exponent. Here, $\dot{\bar{\epsilon}}_0 = 10^3\,\mathrm{s}^{-1}$ and $m = 0.025$. The temperature dependence specified through the function $G(\Theta)$ might depend on the material. In all calculations, the following form has been adopted

$$G(\Theta) = 1 + b\exp\left[-c(\Theta_0 - 273)\right]\left\{\exp\left[-c(\Theta - \Theta_0)\right] - 1\right\} \tag{8}$$

with b and c being material parameters and Θ and Θ_0 being given in Kelvin. Θ_0 is a reference temperature. A criterion for cleavage is used, which is based on a material dependent critical stress, σ_c, over a critical distance [6]. A plane strain model of the Charpy V-notch specimen is analyzed. For the standard specimen, the dimensions are $L = 55$mm, $B = 10$mm, $D = 2$mm, $R = 0.25$mm, $A = 40$mm and $\psi = 22.5^\circ$; see Fig. 1.

EXPERIMENTAL DATA

Charpy impact tests were conducted on two pipe steels which differ in both inclusion content and yield strength. Steel **A** is a low strength isotropic sheet with $\sigma_0 = 322$MPa along the transverse direction T, which contains mainly rounded manganese sulfide inclusions MnS with a volume fraction of 0.00186. Steel **H** is a hot–rolled sheet with $\sigma_0 = 500$MPa along T, and containing MnS stringers with an estimated volume fraction of 0.0004 along with some equiaxed oxide particles whose volume fraction is less than 0.0002. The presence of the elongated MnS inclusions results in directionality of the fracture properties. For instance, the upper shelf energy is about $106\mathrm{J/cm}^2$ in the loading configuration T–L, which is half the value measured for the L–T loading configuration. In addition, steel **H** has a low ductile-brittle transition temperature (DBTT) of about -138°C whereas steel **A** has a DBTT of about -12°C.

Although steel **A** is softer than **H**, it exhibits higher strain hardening with $N = 0.25$, while $N = 0.12$ in steel **H**. Also, tensile tests on smooth specimens were carried out at various temperatures in steel **H**. In the

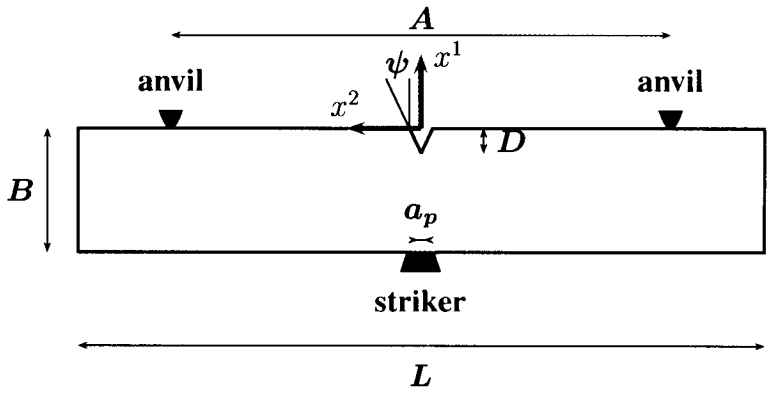

Figure 1: Geometry of the Charpy specimen with prescribed boundary conditions.

range 100°Cto 500°C, the rate of decrease of the yield strength is about 30 MPa every 100°C. This rate is representative of pipe steels with a ferrite–pearlite microstructure and hence applies to steel **A** as well. In addition, the increase in strength at -196°C may depend on the steel. The ratio $g(\epsilon_0, -196°C)/g(\epsilon_0, \Theta_0)$ was found to be equal to 2 for steel **H**. The same value is used for steel **A**. These data are enough to identify the thermal softening law (8) and the values $b = 0.2068$, $c = 0.009$ and $\Theta_0 = 273$K were then used for both materials.

Three geometries were tested in the T–L configuration for each steel. Each geometry is denoted CVNx where x refers to the value of specimen's width B; see Figure 1. The CVN10 specimen is the standard ASTM specimen. The notch depth D was also varied such that the ratio D/B was kept constant. It was found that the normalized upper shelf energy (USE) decreases with decreasing ligament size for both steels, with the decrease rate being enhanced in steel **H**. For example, USE values for the ASTM and CVN3 specimens were 106J/cm^2 and 66.5J/cm^2 respectively in steel **H** whereas they were 82J/cm^2 and 62.7J/cm^2 respectively in steel **A**. Most importantly, varying ligament size was found to affect the ductile to brittle transition temperature (DBTT) in steel **A** but not significantly in steel **H**. Halving the ligament size decreased the DBTT from -12°C to -31°C in steel **A**.

NUMERICAL RESULTS

For both steels, results are shown for two of the tested geometries: ASTM and CVN5. In the case of steel **H**, additional results are presented for a double size specimen, CVN20, for comparison. Typical meshes used in the simulations are shown in Figure 2. For a given material, the same finite element size was used for all specimen sizes in the region close to the notch. The element size, set equal to the average inclusion spacing

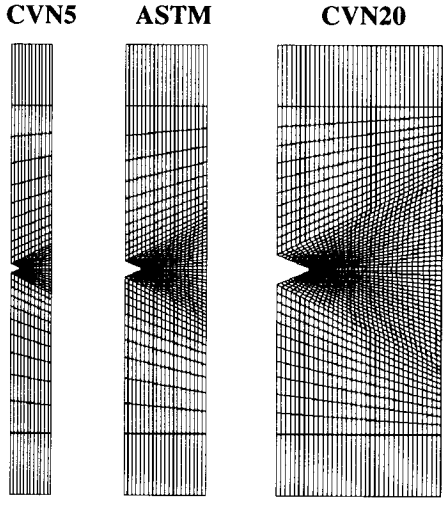

Figure 2: Typical finite element meshes used for steel **H**.

in the plane T–L, is about 240μm in steel **H** and 300μm in steel **A**. To confirm such values, quantitative metallography is under progress. The initial porosity is identified with the inclusion volume fraction assuming that instantaneous nucleation occurs uniformly at low strain. This is a reasonable approximation in steel **H** since the orientation of the major stress is perpendicular to the main inclusion length. In steel **A**, nucleation can be accounted for as in [7]. Corresponding results are presented elsewhere. Here, $f_0 = 0.0006$ in steel **H** and $f_0 = 0.002$ in steel **A**.

In order not to bias the numerical results towards the experimental data, the model parameters for ductile failure, f_c and f_f, are inferred from predictive approaches for coalescence [8, 9]. These have shown quite reasonable agreement with micromechanical unit–cell calculations [10, 11]. Assuming for the inclusions an initial isotropic distribution, the porosity at coalescence is $f_c = 0.018$ and $f_c = 0.022$ in steels **H** and **A** respectively, at an average stress triaxiality ratio of 2. The porosity at failure is $f_f = 0.10$ in **H** and $f_f = 0.17$ in **A**. These values of f_f are based on $q_1 = 1.35$ and $q_1 = 1.15$ for steels **H** and **A** respectively. As in [10], these values account for a strain hardening effect on void growth rates. It is difficult to infer the critical stress for cleavage from experimental measurements. Hence, the values $\sigma_c = 2450\,\mathrm{MPa}$ and $\sigma_c = 2025\,\mathrm{MPa}$ were used in steels **H** and **A** respectively to calibrate the DBTT in the ASTM specimen.

Figure 3 shows selected curves of normalized force plotted against imposed displacement. For each specimen and steel, the curves shown are representative of the upper and lower shelves together with the transition domain. Let us focus first on the lower shelf and transition range. In the ASTM specimens of both steels, Figs 3(a) and (c), the cleavage stress is attained shortly after initial yielding right at the notch tip, while the overall response is still linear. In the CVN5 specimens, however, general yielding slightly precedes the onset

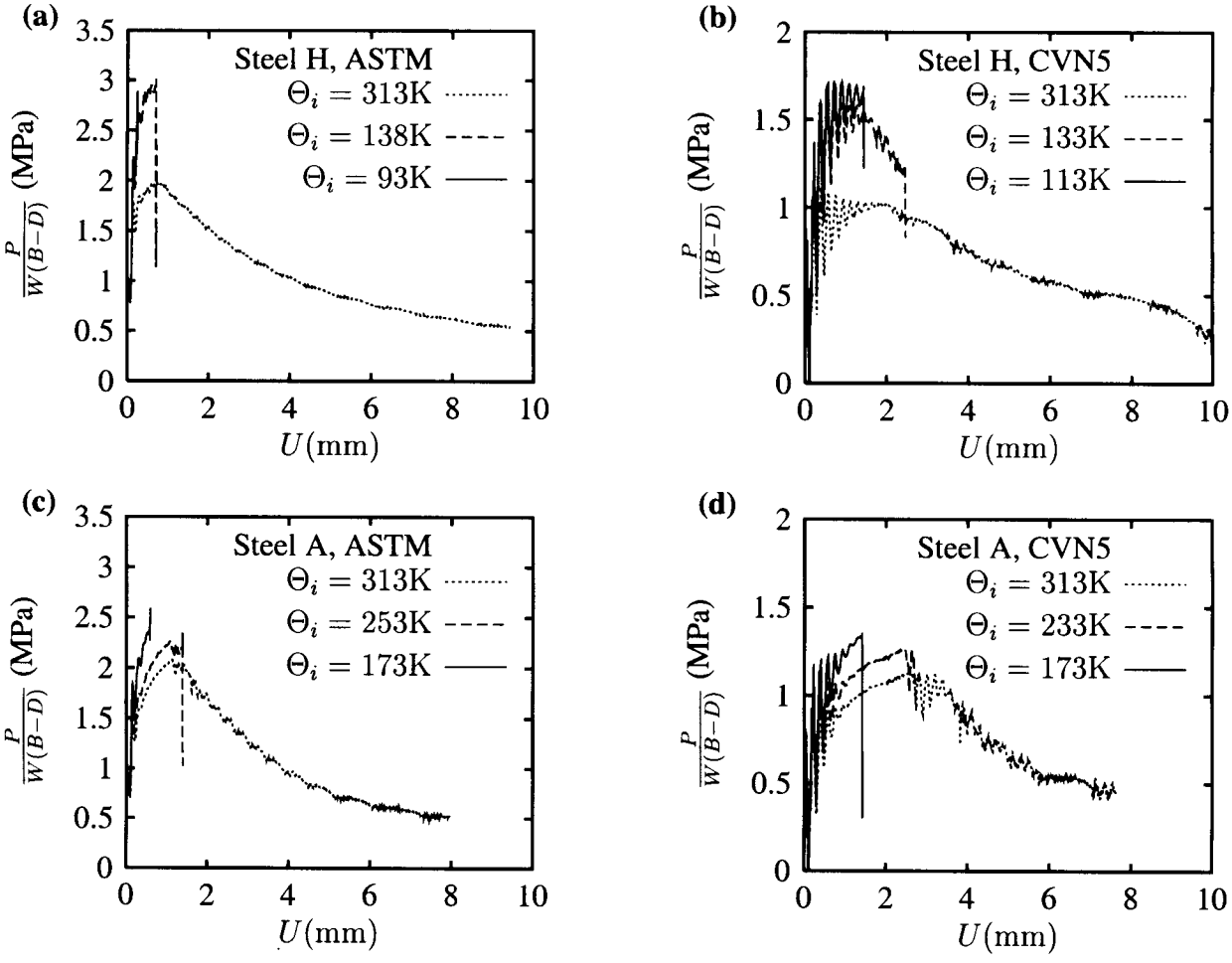

Figure 3: Representative curves of force, P, *vs* imposed displacement, U, for steel **H** and ASTM–specimen (a) or CVN5–specimen (b) and for steel **A** and ASTM–specimen (c) or CVN5–specimen (d).

of cleavage such that large bending of the specimen is observed, Figs 3(b) and (d). Moreover, cleavage does

not initiate at the notch root but at a distance of about five element sizes away from it. At higher temperatures, i.e. $\Theta_i = 313$K, plasticity spreads from the notch root to the opposite free surface and large scale yielding conditions are met. Pure ductile fracture then occurs across the specimen width. Calculations are terminated at $U = 9.5$mm and $U = 8$mm in the case of steels **H** and **A** respectively.

From the force, P, and the displacement, U, the total energy absorbed is computed. This is done for each initial temperature to obtain the computed transition curve. Absorbed energy versus initial temperature curves are shown for steel **H** in Figure 4 where results for the CVN20 specimen are also reported. A comparison with experimental results is shown in Table 1 for both steels in terms of the transition temperature and the upper shelf energy normalized by ligament area, K_{CV}. For steel **A**, the experimental shift in DBTT with ligament size is well reproduced. Increasing the ligament size is expected to have the following implications: (i) it increases the stress level through inertia; (ii) it increases the bending moment which tends to raise the strain level near the notch which leads to more thermal softening and (iii) increasing the ligament size decreases the nominal strain rate within the specimen. The effect of inertia is to increase the DBTT when the ligament size increases whereas the lower strain rate acts in the other direction. The increased bending moment increases the stress level which would tend to decrease the DBTT but it also increases the strain level which tends to increase the DBTT. For steel **A** the increase in stress largely due to inertia appears to be the dominant effect.

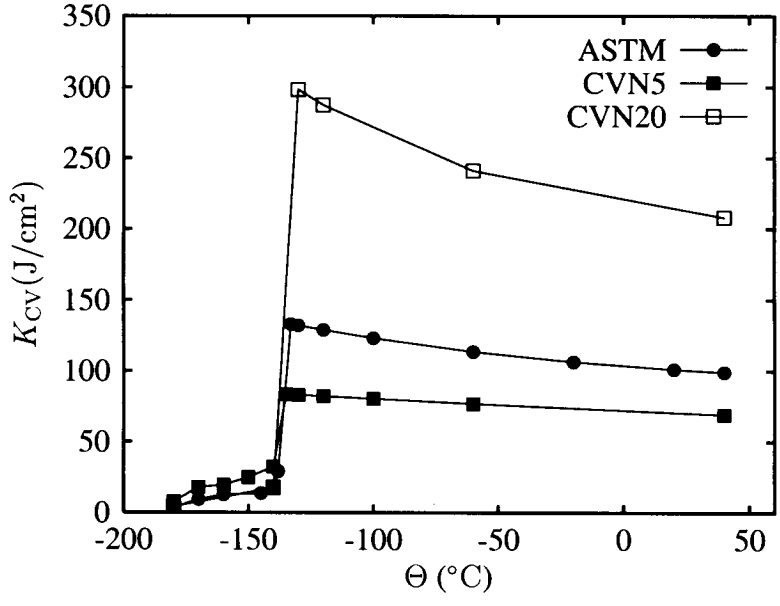

Figure 4: Calculated transition curves in steel **H** for three specimen geometries.

On the other hand, there is no shift of the DBTT in steel **H**, Fig. 4, which matches the experimental trend. In fact, the DBTT measured in specimen CVN3, not shown, is about -130°C, which is almost the same as for the ASTM specimen. Careful investigation of the numerical results shows that the thermal softening effect is here much more important than for steel **A** within the transition range. Indeed, at $\Theta_i = 133$K, the increase in temperature at the notch root is about 65 K in the CVN5 specimen, much lower than the $\Delta\Theta \approx 250$K encountered in a standard specimen at an approximately similar displacement. This counterbalances the effect of inertia and explains the trend in Figure 4.

The upper shelf energies are reasonably well reproduced, although the agreement in the case of steel **A** might be improved. As in the experiments, K_{CV} increases with increasing size. This is due to more plastic dissipation in the larger specimens. The fact that K_{CV} is size–dependent confirms that special care has to be taken when extrapolating Charpy V-notch energies to toughness predictions.

TABLE 1: EFFECTS OF LIGAMENT SIZE IN STEELS **H** AND **A**.

Specimen	DBTT (°C)		K_{CV}(J/cm^2)	
	exp.	calc.	exp.	calc.
H, ASTM	-138	-134	106	102
H, CVN5	-108	-136	77.1	78.5
A, ASTM	-12	-17	82.0	91.9
A, CVN5	-31	-27	65.8	60.8

CONCLUSIONS

Ligament size effects were investigated experimentally and numerically on two pipe steels. Full dynamic analyses were carried out. The upper shelf energy decreases with increasing size in general and this is due to the increased plastic dissipation in large specimens. The shift in the DBTT is found to depend on a subtle interplay between inertial effects and thermal softening effects. Steel **H** had a much lower transition temperature than steel **A** because of a higher resistance to cleavage initiation. As a consequence, thermal softening was more significant for steel **H** in the transition range because the softening law in ferritic–pearlitic steels exhibits a higher gradient at low temperatures. For both steels, the results give clear evidence of the effects of inertia in the Charpy V-notch test.

Acknowledgements

Support from the Office of Naval Research through grant N00014-97-1-0179 is gratefully acknowledged.

References

[1] A. L. Gurson. *J. Eng. Mat. Tech.*, 99:2–15, 1977.

[2] J. Pan, M. Saje, and A. Needleman. *Int. J. Frac.*, 21:261–278, 1983.

[3] V. Tvergaard. *Int. J. Frac.*, 17:389–407, 1981.

[4] V. Tvergaard. *Int. J. Frac.*, 18:237–252, 1982.

[5] V. Tvergaard and A. Needleman. *Acta metall.*, 32:157–169, 1984.

[6] R. O. Ritchie, J. F. Knott, and J. R. Rice. *J. Mech. Phys. Solids*, 21:395–410, 1973.

[7] A. Needleman and V. Tvergaard. *Int. J. Frac.*, 101:73–97, 2000.

[8] A. A. Benzerga, J. Besson, and A. Pineau. *J. Eng. Mat. Tech.*, 121(2):221–229, 1999.

[9] A. A. Benzerga. PhD thesis, Ecole des Mines de Paris, March 2000. parts in english.

[10] J. Koplik and A. Needleman. *Int. J. Solids Structures*, 24(8):835–853, 1988.

[11] T. Pardoen and J. W. Hutchinson. *J. Mech. Phys. Solids*, 2000. submitted.